

Electron structure and magneto-optics of ferromagnetic 3d metals

Yu. A. Uspenskii and S.V. Khalilov

P.N. Lebedev Physics Institute, Academy of Sciences of the USSR, Moscow
(Submitted 5 September 1988)

Zh. Eksp. Teor. Fiz. **95**, 1022–1036 (March 1989)

The dynamic conductivity tensor $\hat{\sigma}(\omega)$ of ferromagnetic 3d metals is considered analytically and calculated numerically. Such a procedure reveals those features of the $\sigma_{\alpha\beta}(\omega)$ curves which are related directly to such characteristics of the electron spectrum as the width of the *d* band or the magnitudes of the spin-orbit and exchange splittings. The behavior of $\sigma_{\alpha\beta}(\omega)$ in the infrared frequency range is determined by three principal mechanisms of interband transitions, which are of universal nature. All these mechanisms give rise to singularities at energies $\hbar\omega$ of the order of the spin-orbit splitting. In the visible and ultraviolet parts of the spectrum the off-diagonal components of the conductivity tensor are proportional to the difference between the diagonal components with opposite spins, which makes magneto-optic effects more sensitive to the spin structure. The interval between singularities of opposite signs at the edge of the visible spectrum carries information on the exchange splitting and the point of reversal of the sign—on the width of the valence subband with the up spin. The results obtained are practically independent of the crystal structure.

INTRODUCTION

Optical measurements represent one of the main sources of information on the electron structure of metals. In the case of ferromagnets, studies of their optical properties provide an even richer material because observations of the magneto-optic Faraday, Kerr, and Cotton-Mouton effects used to determine the off-diagonal components of the conductivity tensor $\sigma_{\alpha\beta}(\omega)$. The weakest point is the interpretation of the frequency dependences and establishment of a relationship between the positions of the main features of the dependences $\sigma_{\alpha\beta}(\omega)$ and the parameters of the electron structure of a metal. Attempts to analyze the expression for the conductivity using the spin-orbit splitting as a parameter was made back in the fifties.¹ Introduction of a number of simplifying assumptions enabled Argyres¹ to obtain a relationship between the off-diagonal and diagonal components of $\sigma_{\alpha\beta}(\omega)$. Experimental investigations²⁻⁴ demonstrated however that this relationship is obeyed well only in a certain range of frequencies, whereas elsewhere it is completely invalid. Subsequent interpretations of the experimental results have been based either on a purely phenomenological approach⁵ or on speculative assumptions about the relationship of some particular feature of $\sigma_{\alpha\beta}(\omega)$ to a specific group of interband transitions involving "additional" mechanisms.² Finally, calculations of magneto-optic properties from "first principles" reported in Ref. 6 provided on the whole a satisfactory description of the experimental results. It follows that the existing difficulties are not of fundamental nature and are simply due to failure to establish the complex relationship between the electron structure and optical properties of ferromagnets.

We shall attempt to explain the main features of the $\sigma_{\alpha\beta}(\omega)$ curves and to establish their relationship to such characteristics of the electron structure as the width of the *d* band or the magnitudes of the spin-orbit and exchange splittings. We shall therefore use the "first principles" approach in a relativistic calculation of all the components of the conductivity tensor of iron, cobalt, and nickel. The results will be employed to construct simple models based on the elec-

tron structure of ferromagnetic 3d metals and describing the behavior of $\sigma_{\alpha\beta}(\omega)$ in the infrared, visible, and ultraviolet parts of the spectrum. A combined analysis of the off-diagonal and diagonal components of $\sigma_{\alpha\beta}(\omega)$ will make it possible to check the models against the results of magneto-optic and conventional optical measurements, and to establish the relationships between the main features of the off-diagonal and diagonal components of the conductivity.

1. FREQUENCY DEPENDENCE OF THE CONDUCTIVITY TENSOR

It is known⁷ that the magneto-optic effects are due to the difference between the complex refractive indices of light with left- and right-handed polarizations (\tilde{n}_l and \tilde{n}_r). Thus, the angle of rotation of the plane of polarization in the Faraday effect is

$$\alpha_F = \frac{\omega d}{2c} \operatorname{Re}(\tilde{n}_r - \tilde{n}_l), \quad \tilde{n}_{r,l} = \left[1 + i \frac{4\pi\sigma_{r,l}(\omega)}{\omega} \right]^{1/2}, \quad (1)$$

where *d* is the thickness of the plate and *c* is the velocity of light. In the case of a cubic ferromagnetic metal with a magnetic moment directed along the *z* axis the left-handed (−) and the right-handed (+) components of the conductivity are given by

$$\sigma_{r,l}(\omega) = \sigma_{xx}(\omega) \pm i\sigma_{xy}(\omega). \quad (2)$$

We can see from Eqs. (1) and (2) that the magneto-optic effects are determined by the off-diagonal components of $\sigma_{\alpha\beta}(\omega)$, i.e., by the anisotropy of the motion of electrons in the coordinate space. Such an anisotropy appears in the presence of an external magnetic field because electrons follow paths around the lines of force of the magnetic field. The presence of a spontaneous spin moment in a nonrelativistic ferromagnet has no effect on the motion of an electron in the coordinate space. The motion of electrons becomes anisotropic only if the Hamiltonian includes the spin-orbit interaction linking the spatial and spin degrees of freedom. In other words, if a metal is not subjected to an external magnetic field, the magneto-optic effects can appear if both ferro-

magnetism and the spin-orbit interaction are present.

We shall describe the motion of an electron confining ourselves to relativistic corrections $\sim v^2/c^2$, i.e., we shall assume that the wave function satisfies the Schrödinger equation:

$$\left\{ \left[\frac{p^2}{2m} + V_{eff}(r) \right] \delta_{ss'} + \frac{\hbar^2}{4m^2 c^2} [\nabla V_{eff} \mathbf{p}] \sigma_{ss'} \right\} \psi_s^{k\lambda}(r) = E_{k\lambda} \psi_s^{k\lambda}(r). \quad (3)$$

In the random-phase approximation without allowance for the local field effects, we find that the real and imaginary parts of the conductivity tensor are

$$\begin{aligned} \text{Re } \sigma_{\alpha\beta}(\omega) &= \frac{\pi e^2}{2} \delta(\omega) \sum_{k\lambda} \delta(E_{k\lambda} - E_F) \text{Re} [j_\alpha^{k\lambda}(\mathbf{k}) j_\beta^{k\lambda}(\mathbf{k})] \\ &+ \hbar e^2 \sum_{k\lambda \neq k'\lambda'} f_{k\lambda} (1 - f_{k'\lambda'}) \left\{ \text{Im} [j_\alpha^{k\lambda'}(\mathbf{k}) j_\beta^{k'\lambda}(\mathbf{k})] \frac{P}{\hbar^2 \omega^2 - E_{k\lambda'}^2(\mathbf{k})} \right. \\ &\quad \left. + \text{Re} [j_\alpha^{k\lambda'}(\mathbf{k}) j_\beta^{k'\lambda}(\mathbf{k})] \pi \frac{\delta(\hbar\omega - E_{k\lambda'}(\mathbf{k}))}{2\hbar\omega} \right\}, \quad (4) \\ \text{Im } \sigma_{\alpha\beta}(\omega) &= \frac{e^2}{\omega} \sum_{k\lambda} \delta(E_{k\lambda} - E_F) \text{Re} [j_\alpha^{k\lambda}(\mathbf{k}) j_\beta^{k\lambda}(\mathbf{k})] \\ &+ \hbar e^2 \sum_{k\lambda \neq k'\lambda'} f_{k\lambda} (1 - f_{k'\lambda'}) \left\{ \text{Re} [j_\alpha^{k\lambda'}(\mathbf{k}) j_\beta^{k'\lambda}(\mathbf{k})] \frac{P}{\hbar^2 \omega^2 - E_{k\lambda'}^2(\mathbf{k})} \right. \\ &\quad \left. \times \frac{E_{k\lambda'}(\mathbf{k})}{\hbar\omega} + \text{Im} [j_\alpha^{k\lambda'}(\mathbf{k}) j_\beta^{k'\lambda}(\mathbf{k})] \pi \frac{\delta(\hbar\omega - E_{k\lambda'}(\mathbf{k}))}{2\hbar\omega} \right\}, \quad (5) \\ j_\alpha^{k\lambda}(\mathbf{k}) &\equiv \frac{1}{m} \left\langle k\lambda \left| \hat{p}_\alpha + \frac{\hbar}{4mc^2} [\sigma \nabla V_{eff}]_\alpha \right| k\lambda \right\rangle, \end{aligned}$$

where $E_{k\lambda}(\mathbf{k}) \equiv E_{k\lambda} - E_{k\lambda'}$; $|k\lambda\rangle$ is a one-electron state in a band λ , described by Eq. (3); $f_{k\lambda}$ are occupation numbers. The first terms in Eqs. (4) and (5) are governed by intra-band excitations of electrons and the other terms by inter-band excitations. Since $\text{Im } \sigma_{\alpha\beta}(\omega)$ and $\text{Re } \sigma_{\alpha\beta}(\omega)$ are linked by the Kramers-Kronig dispersion relationships, it is sufficient to calculate one of these two quantities, for example $\text{Re } \sigma_{\alpha\alpha}(\omega)$ or $\text{Im } \sigma_{\alpha\beta}(\omega)$ ($\alpha \neq \beta$), which makes it possible to find the other quite readily by integration with respect to ω .

It is known that $\text{Re } \sigma_{\alpha\beta}(\omega)$ satisfies the sum rule:

$$\int_0^\infty d\omega \text{Re } \sigma_{\alpha\beta}(\omega) = \pi N e^2 \delta_{\alpha\beta} / 2m.$$

Describing $\text{Re } \sigma_{\alpha\beta}(\omega)$ by means of Eq. (4), we obtain

$$\begin{aligned} &\frac{\pi e^2}{2} \sum_{k\lambda} \delta(E_{k\lambda} - E_F) \text{Re} [j_\alpha^{k\lambda}(\mathbf{k}) j_\beta^{k\lambda}(\mathbf{k})] \\ &+ \frac{\pi e^2}{2} \sum_{k\lambda \neq k'\lambda'} \frac{f_{k\lambda} (1 - f_{k'\lambda'})}{E_{k\lambda'}(\mathbf{k})} \text{Re} [j_\alpha^{k\lambda'}(\mathbf{k}) j_\beta^{k'\lambda}(\mathbf{k})] = \frac{\pi N e^2}{2} \delta_{\alpha\beta}. \quad (6) \end{aligned}$$

The symmetry imposes major limitations on the nature of the tensor $\sigma_{\alpha\beta}(\omega)$ of cubic crystals. For example, when the spin moment orientations are $\mathbf{M} \parallel [001]$ and $\mathbf{M} \parallel [110]$, we find that

$$\sigma_{\alpha\beta}^{[001]} = \begin{pmatrix} \sigma_{xx} & \sigma_{xy} & 0 \\ -\sigma_{xy} & \sigma_{xx} & 0 \\ 0 & 0 & \sigma_{zz} \end{pmatrix}, \quad \sigma_{\alpha\beta}^{[110]} = \begin{pmatrix} \sigma_{xx} & \sigma_{xy} & \sigma_{xz} \\ \sigma_{xy} & \sigma_{xx} & -\sigma_{xz} \\ -\sigma_{xz} & \sigma_{xz} & \sigma_{zz} \end{pmatrix}, \quad (7)$$

where the components $\text{Im } \sigma_{\alpha\beta}$ ($\alpha \neq \beta$) antisymmetric relative to $\alpha \rightleftharpoons \beta$ are

$$\begin{aligned} \text{Im } \sigma_{\alpha\beta}(\omega) &= \frac{\pi e^2}{2\omega} \sum_{k\lambda \neq k'\lambda'} \delta(\hbar\omega - E_{k\lambda'}(\mathbf{k})) f_{k\lambda} (1 - f_{k'\lambda'}) \\ &\quad \times \text{Im} [j_\alpha^{k\lambda'}(\mathbf{k}) j_\beta^{k'\lambda}(\mathbf{k})], \quad (8) \end{aligned}$$

and the symmetric components $\text{Re } \sigma_{\alpha\beta}$ ($\alpha \neq \beta$) are given by

$$\begin{aligned} \text{Re } \sigma_{\alpha\beta}(\omega) &= \frac{\pi e^2}{2} \delta(\omega) \sum_{k\lambda} \delta(E_{k\lambda} - E_F) \text{Re} [j_\alpha^{k\lambda}(\mathbf{k}) j_\beta^{k\lambda}(\mathbf{k})] \\ &+ \frac{\pi e^2}{2\omega} \sum_{k\lambda \neq k'\lambda'} \delta(\hbar\omega - E_{k\lambda}(\mathbf{k})) f_{k\lambda} (1 - f_{k'\lambda'}) \text{Re} [j_\alpha^{k\lambda'}(\mathbf{k}) j_\beta^{k'\lambda}(\mathbf{k})]. \quad (9) \end{aligned}$$

As in the presence of an external magnetic field, the symmetric components $\sigma_{\alpha\beta}$ are even functions of \mathbf{M} , whereas the antisymmetric components are odd functions. More vigorously, the symmetric and antisymmetric components are proportional respectively to the even and odd powers of the parameter

$$\gamma = \frac{2\bar{\xi}}{\Delta E_{\lambda\lambda'}} \frac{n_+ - n_-}{n_+},$$

where $2\bar{\xi}$ is the average value of the spin-orbit splitting and $\Delta E_{\lambda\lambda'}$ is the average value of $E_{\lambda\lambda'}$ for bands with the same spin direction. Assuming that $2\bar{\xi} \approx 0.2$ eV, $\Delta E_{\lambda\lambda'} \approx W_d / 5 \approx 1$ eV (W_d is the width of the d band), and $(n_+ - n_-) / n_+ \sim 1/3$, we find that $\gamma \sim 1/15$. For example, if the direction of the moment is $\mathbf{M} \parallel [110]$, the characteristic quantities σ_{xx} , σ_{xz} , and σ_{xy} should be in the ratio of unity, γ and γ^2 , in satisfactory agreement with the experimental results.^{2-4,8}

The Faraday effect is determined solely by the antisymmetric components of $\sigma_{\alpha\beta}$. The absorption of light is governed by the expression⁹

$$Q = \frac{1}{4\pi} \langle E \partial D / \partial t \rangle_t = 1/2 \text{Re} [\sigma_{\alpha\beta} E_\alpha^* E_\beta]. \quad (10)$$

If $\mathbf{M} \parallel [001]$, the absorption of light is described by $\text{Re } \sigma_{\alpha\alpha}$ and $\text{Im } \sigma_{xy}$, whereas for $\mathbf{M} \parallel [110]$, it is described by $\text{Re } \sigma_{\alpha\alpha}$, $\text{Re } \sigma_{xy}$, and $\text{Im } \sigma_{xz}$. For an arbitrary direction of \mathbf{M} the tensor $\sigma_{\alpha\beta}$ includes both even and odd (in respect of \mathbf{M}) off-diagonal components. The absorption of light is then determined by the real parts of the symmetric components of $\sigma_{\alpha\beta}$ (even in \mathbf{M}) and by the imaginary parts of the antisymmetric components (odd in \mathbf{M}).

2. ANALYSIS OF $\sigma_{\alpha\beta}(\omega)$ USING PERTURBATION THEORY

In this section we shall study the frequency dependence of $\sigma_{xy}(\omega)$ when $\mathbf{M} \parallel [001]$ and we shall do this applying perturbation theory to the spin-orbit interaction (SOI). In contrast to earlier investigations,^{5,10} we shall allow for the characteristic features of the electron structure of ferromagnetic 3d metals, which makes it possible to formulate quite realistic models describing the behavior of $\sigma_{\alpha\beta}(\omega)$ in the visible

and ultraviolet parts of the spectrum and also when $\hbar\omega \sim 2\bar{\xi}$.

In the lowest order of perturbation theory the relativistic wave functions $|\mathbf{k}\lambda\rangle$ are linear combinations of the non-relativistic wave functions $|\mathbf{k}m\sigma\rangle$:

$$|\mathbf{k}\lambda\rangle = |\mathbf{k}m\sigma\rangle + \sum_l' \frac{\langle \mathbf{k}l\sigma' | \hat{H}_{s0} | \mathbf{k}m\sigma \rangle}{E_{\mathbf{k}m\sigma} - E_{\mathbf{k}l\sigma'}} |\mathbf{k}l\sigma'\rangle, \quad (11)$$

where σ is the spin projection and

$$\hat{H}_{s0} = \frac{1}{2m^2c^2} \frac{1}{r} \frac{dV}{dr} (\sigma l) \equiv \xi(r) (\sigma l)$$

is the SOI operator. Equation (11) is invalid in the vicinity of degeneracy points, where

$$|E_{\mathbf{k}m\sigma} - E_{\mathbf{k}l\sigma'}| \lesssim 2\bar{\xi}.$$

However, if $\hbar\omega \sim 2\bar{\xi}$, regions in the vicinity of these points represent a negligible fraction of the phase space and their contribution can be ignored. Substituting Eq. (11) into Eq. (5), and confining ourselves to the terms

$$\sim \nu = \frac{2\bar{\xi}}{\Delta E} \frac{n_\uparrow - n_\downarrow}{n_\uparrow}$$

we obtain

$$\begin{aligned} \text{Im } \sigma_{xy}(\omega) &= \frac{\pi e^2}{\hbar\omega m^2} \sum_{\mathbf{k}m'\sigma} \{ F_{m'\sigma}^{xy}(\mathbf{k}) f_{\mathbf{k}m'\uparrow} (1 - f_{\mathbf{k}m'\downarrow}) \\ &\quad \times \delta(\hbar\omega - E_{m'\sigma}(\mathbf{k})) \\ &\quad - F_{m'\sigma}^{xy}(\mathbf{k}) f_{\mathbf{k}m'\downarrow} (1 - f_{\mathbf{k}m'\uparrow}) \delta(\hbar\omega - E_{m'\sigma}(\mathbf{k})) \}, \quad (12) \\ F_{m'\sigma}^{xy}(\mathbf{k}) &\equiv 2i \sum_l' \left[\frac{L_{lm'}^{xy}}{E_{m'l}} p_x^{lm'} p_y^{m'm} + \frac{L_{lm'}^z}{E_{m'l}} p_x^{lm'} p_y^{m'm} \right]. \quad (13) \end{aligned}$$

Here,

$$L_{m'n\sigma}^z \equiv \langle \mathbf{k}m\sigma | \xi(r) \hat{l}_z | \mathbf{k}n\sigma \rangle, \quad p_\alpha^{mn\sigma}(k) \equiv \langle \mathbf{k}m\sigma | p_\alpha | \mathbf{k}n\sigma \rangle.$$

The SOI components proportional to $\hat{\sigma}_x$ and $\hat{\sigma}_y$, which result in spin flip, are missing from Eq. (11) because their contribution to $\text{Im } \sigma_{xy}$ is of the order of γ^3 .

Before analyzing the frequency dependence of Eq. (12), we shall list briefly the main features of the electron structure of ferromagnetic 3d metals Fe, Co, and Ni. In all these metals the Fermi level is near the top edge of the d band with the up spin or in the upper half of the d band with the down spin. The total width of the d band with one spin direction, which includes five subbands, ranges from 6.2 eV for Fe to 5.2 eV for Ni, whereas the exchange splitting ranges from 2 eV for Fe to 0.5 eV for Ni. The s and p bands are located respectively below and above the d band (more accurately, these are the hybridized sp bands with large fractions of the s or p states). The exchange splitting for these bands is 4–5 times less than for the d band, and the density of the electron states is several times less. The investigated frequency range can be split conveniently into three intervals: a) $2\bar{\xi} \ll \hbar\omega < W_d$, b) $\hbar\omega > W_d$, c) $\hbar\omega \sim 2\bar{\xi}$.

a) At frequencies $2\bar{\xi} \ll \hbar\omega < W_d$ the states m and m' and the majority of the l states in Eqs. (12) and (13) belong to the d band. In this case the spin direction has very little effect on the difference between the energies $E_{m'\sigma}$, $E_{m\sigma}$, and

$E_{m'\sigma}$ or on the magnitude of the matrix elements $L_{m'l\sigma}^z$ and $L_{m'l\sigma}^z$ (the average deviation does not exceed 5%). We can therefore quite accurately assume that $F_{m'\sigma}^{xy} = F_{m'\sigma}^{xy} \equiv F_{d'd}^{xy}$. This simplifies greatly Eq. (12), which now becomes

$$\begin{aligned} \text{Im } \sigma_{xy}(\omega) &\approx \frac{\pi e^2}{\hbar\omega m^2} \sum_{\mathbf{k}d \neq d'} F_{d'd}^{xy}(\mathbf{k}) \delta(\hbar\omega - E_{dd'}(\mathbf{k})) \\ &\quad \times [f_{\mathbf{k}d'\uparrow} (1 - f_{\mathbf{k}d\uparrow}) - f_{\mathbf{k}d'\downarrow} (1 - f_{\mathbf{k}d\downarrow})]. \end{aligned}$$

We can easily see that exactly the same factor $\delta(\hbar\omega - E_{dd'}) f_{d'\sigma} (1 - f_{d\sigma})$ occurs in the familiar nonrelativistic expressions of the diagonal components of the conductivity $\text{Re } \sigma_{xx}(\omega)$ and $\text{Re } \sigma_{yy}(\omega)$. Therefore, if $2\bar{\xi} \ll \hbar\omega < W_d$, the quantity $\text{Im } \sigma_{xy}(\omega)$ is proportional to the difference $\text{Re } \sigma_{yy}(\omega) - \text{Re } \sigma_{xx}(\omega)$. This can be demonstrated by inspection of the frequency dependences of $\omega \text{Im } \sigma_{xy}(\omega)$, $\text{Re } \sigma_{xx}(\omega)$, and $\text{Re } \sigma_{yy}(\omega)$ found numerically (see Figs. 7 and 8 below).

b) At frequencies $\hbar\omega \gtrsim W_d$ (of the order of the width of the valence band) the occupied states λ' are dominated by the lower $1\uparrow$ and $1\downarrow$ bands, which are s -type bands. Since the unoccupied states λ are dominated by the states near the top of the d band, Eq. (12) can be written in the form

$$\begin{aligned} \text{Im } \sigma_{xy}(\omega) &\approx \frac{\pi e^2}{\hbar\omega m^2} \sum_{\mathbf{k}} F_{sd}^{xy}(\mathbf{k}) [\delta(\hbar\omega - E_{ds\uparrow}(\mathbf{k})) f_{\mathbf{k}s\uparrow} (1 - f_{\mathbf{k}d\downarrow}) \\ &\quad - \delta(\hbar\omega - E_{ds\downarrow}(\mathbf{k})) f_{\mathbf{k}s\downarrow} (1 - f_{\mathbf{k}d\downarrow})]. \quad (14) \end{aligned}$$

We can see that if

$$\hbar\omega \approx \frac{1}{2}(E_{ds\uparrow} + E_{ds\downarrow}),$$

The $\text{Im } \sigma_{xy}(\omega)$ curve changes its sign with peaks of opposite signs at energies

$$\hbar\omega_1 = \langle E_{ds\uparrow} \rangle \approx W_d, \quad \hbar\omega_2 = \langle E_{ds\downarrow} \rangle \approx W_d + 2\Delta_{xc}^d.$$

The separation between these peaks is approximately equal to the average splitting $2\Delta_{xc}^d$ of the d band and the point of reversal of the sign corresponds to the energy $W_d + \Delta_{xc}^d$ (we have ignored here a weak exchange splitting of the s band).

c) In the infrared frequency range characterized by $\hbar\omega \sim 2\bar{\xi}$ (which is of the order of the spin-orbit splitting energy) an analysis of the behavior of $\text{Im } \sigma_{xy}(\omega)$ is more difficult. We can distinguish three main contributions to $\text{Im } \sigma_{xy}(\omega)$:

I) from regions where the nonrelativistic sheets of the Fermi surface m' and $m\sigma$ (i.e., the sheets with the same direction of the spin) approach to a distance $\Delta k \lesssim 2\bar{\xi}/v_F$;

II) from the vicinities of the lines of intersection of the $m'\uparrow$ and $m\downarrow$ or $m'\downarrow$ and $m\uparrow$ sheets, which exist for the majority of metals with a spin moment $\mu \equiv n_\uparrow - n_\downarrow \gtrsim 1$;

III) from regions between almost parallel sheets of the Fermi surface $m\uparrow$ and $m\downarrow$, corresponding to a weak exchange splitting $2\Delta_{xc} \sim 2\bar{\xi}$. These situations are shown schematically in Fig. 1.

Case I differs from Eq. (12) only because we now have $E_{m'\sigma} \lesssim 2\bar{\xi}$ and, therefore, hybridization of the bands $m\sigma$ and $m'\sigma$ due to the SOI must be allowed for exactly and not in the first order with respect to $\bar{\xi}$. Simple estimates indicate that in the case of hybridized bands λ' and λ we have

$$\text{Im } \{ \langle \lambda' | p_x | \lambda \rangle \langle \lambda | p_y | \lambda' \rangle \} \sim 1,$$

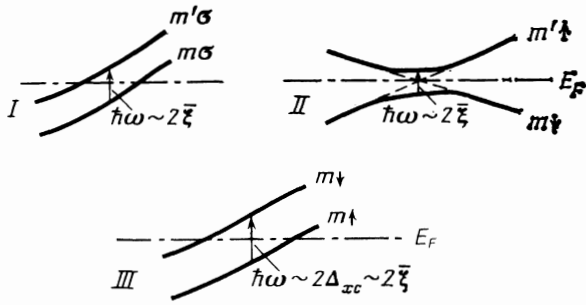


FIG. 1. Distributions of energy bands in the vicinity of the Fermi level, showing the transitions between these bands making the greatest contribution to $\sigma_{\alpha\beta}(\omega)$ at $\hbar\omega \sim 2\xi_{\mathbf{k}}$.

and the total contribution to $\text{Im } \sigma_{xy}(\omega)$ is governed by the volume of the k space, where

$$E_{m\sigma}(\mathbf{k}) > E_F > E_{m'\sigma}(\mathbf{k}), \quad E_{m'\sigma}(\mathbf{k}) - E_{m\sigma}(\mathbf{k}) \ll 2\xi_{\mathbf{k}}$$

In contrast to case I, associated with an accidental approach of the $m\sigma$ and $m'\sigma$ bands near the Fermi level, cases II and III occur in almost all the metals characterized by a spin moment $\mu \gtrsim 1$ or $\mu \ll 1$ respectively. Since the matrix moment of the momentum is diagonal in spin, the contributions to $\text{Re } \sigma_{xx}(\omega)$ appear in these two cases as a result of hybridization of the bands with opposite directions of the spin. A more detailed discussion based on the $\mathbf{k} \cdot \mathbf{p}$ form of perturbation theory yields the following result for case II:

$$\text{Re } \sigma_{xx}^{\text{II}}(\omega) \approx \frac{\pi e^2}{\hbar(2\pi)^3} \oint_L \frac{dl_{\mathbf{k}} |\xi_{\mathbf{k}}|^2}{\hbar\omega (\hbar^2\omega^2 - 4|\xi_{\mathbf{k}}|^2)^{1/2}} \times \frac{|v_x^-(\mathbf{k})|^2 \theta(\hbar\omega - 2|\xi_{\mathbf{k}}|)}{|[v^-(\mathbf{k})v^+(\mathbf{k})]|}, \quad (15)$$

where

$$v^{\pm}(\mathbf{k}) \equiv \frac{1}{2}(v_{m\uparrow}(\mathbf{k}) \pm v_{m\downarrow}(\mathbf{k})), \quad \xi_{\mathbf{k}} \equiv \langle m\uparrow | \hat{H}_{s0} | m\downarrow \rangle,$$

and L is the line of intersection of the nonrelativistic sheets $m\uparrow$ and $m\downarrow$. A distinguishing feature of curve 15 is a sharp maximum at $\hbar\omega \sim 2\xi_{\mathbf{k}}$ (if $\xi_{\mathbf{k}}$ is independent of \mathbf{k} , a square-root singularity is observed) and a steep fall proportional to $1/\omega^2$ at higher energies.

In case III an approximate analytic expression for $\text{Re } \sigma_{xx}(\omega)$ is

$$\text{Re } \sigma_{xx}^{\text{III}}(\omega) \approx \frac{8\pi e^2}{\hbar(2\pi)^3} \oint_S d\mathbf{s}_{\mathbf{k}} \frac{|\xi_{\mathbf{k}}|^2}{\hbar^2\omega^2} \left[1 + \frac{2\Delta_{xc}(\mathbf{k})}{\hbar\omega} \right] \times \delta(\hbar\omega - 2(\Delta_{xc}^2(\mathbf{k}) + |\xi_{\mathbf{k}}|^2)^{1/2}) \frac{|v_x^-(\mathbf{k})|^2}{|v(\mathbf{k})|} \theta(\hbar\omega - 2\Delta_{xc}(\mathbf{k})). \quad (16)$$

Here,

$$\Delta_{xc}(\mathbf{k}) \equiv \frac{1}{2}(E_{m\downarrow}(\mathbf{k}) - E_{m\uparrow}(\mathbf{k})), \quad v_x^-(\mathbf{k}) \equiv \frac{1}{2}(v_{m\uparrow}^x(\mathbf{k}) - v_{m\downarrow}^x(\mathbf{k})), \quad \xi_{\mathbf{k}} \equiv \langle m\uparrow | \hat{H}_{s0} | m\downarrow \rangle.$$

Integration in Eq. (16) is carried out along those parts S of the Fermi surface where the bands $m\uparrow$ and $m\downarrow$ separated on the energy scale by $2\Delta_{xc}(\mathbf{k})$ are almost parallel to one another. In the limit of a weak exchange splitting ($2\Delta_{xc} \sim 2\xi_{\mathbf{k}}$) the ratios $\xi_{\mathbf{k}}/\xi_{\mathbf{k}}$ and $v^-(\mathbf{k})/v(\mathbf{k})$ in Eq. (16) are of the order of $\Delta_{xc}/\Delta E$ (ΔE is the separation to the nearest $m\uparrow$ and $m\downarrow$

bands). Therefore, we can realize case III if interband hybridization of the bands $m\uparrow$ and $m\downarrow$ occurs with other bands, giving rise to dispersion of the exchange splitting $2\Delta_{xc}(\mathbf{k})$. In the opposite case we have $v_x^- \approx \partial\Delta_{xc}(\mathbf{k})/\partial\hbar k_x = 0$ and the effect described as case III disappears.

In the dependence on the relative magnitudes of the exchange and spin-orbit splittings the dominant contribution to $\sigma_{\alpha\beta}(\omega)$ at photon energies $\hbar\omega \sim 2\xi_{\mathbf{k}}$ comes either from case II or case III (in addition to case I). If $\Delta_{xc} \gg \xi_{\mathbf{k}}$, the total length of the lines of intersection of the Fermi surface sheets characterized by the different spins is large, so that

$$\frac{\oint_S dl_{\mathbf{k}}}{\hbar v_{FL}} \bigg/ \oint_S ds_{\mathbf{k}} \gg 1$$

(in this case there are no type III transitions), i.e., at frequencies $\hbar\omega \sim 2\xi_{\mathbf{k}}$ we can expect predominance of type II transitions. As pointed out already, this is typical of iron and cobalt. If $\Delta_{xc} \sim \xi_{\mathbf{k}}$ at the Fermi level, then, in view of the topological similarity between the Fermi surface sheets with different spins separated by the exchange splitting $2\Delta_{xc}$, we have

$$\oint_S ds_{\mathbf{k}} \sim S_F$$

(S_F is the Fermi surface area), i.e.,

$$\frac{\oint_S dl_{\mathbf{k}}}{\hbar v_{FL}} \bigg/ \oint_S ds_{\mathbf{k}} \ll 1$$

(there are practically no type II transitions). Moreover, in the presence of the "third" zone separated from $m\uparrow$ and $m\downarrow$ by $\Delta E \sim \Delta_{xc}$ (which is true of nickel), the quantities occurring in the integral (16) are comparable with the corresponding quantities occurring in Eq. (15). Therefore, if $\Delta_{xc} \sim \xi_{\mathbf{k}}$ and $\Delta E \sim \Delta_{xc}$, the main role is played by type III transitions. Naturally, in addition to the effects described by Eqs. (15) and (16), there are considerable contributions of the "conventional" type I transitions, but they do not exhibit such strong anomalies of the frequency dependence at energies $\hbar\omega \sim 2\xi_{\mathbf{k}}$.

These factors determine the behavior of the off-diagonal component $\text{Im } \sigma_{xy}(\omega)$ in cases II and III. By way of example, we shall give the expression for the contribution made to $\text{Im } \sigma_{xy}(\omega)$ in case II:

$$\text{Im } \sigma_{xy}^{\text{II}}(\omega) \approx \frac{8\pi e^2}{\hbar(2\pi)^3} \oint_L dl_{\mathbf{k}} \frac{\theta(\hbar\omega - 2|\xi_{\mathbf{k}}|) \text{Im } \xi_{\mathbf{k}}}{\hbar\omega (\hbar^2\omega^2 - 4|\xi_{\mathbf{k}}|^2)^{1/2}} \times \sum_i' \left\{ \left[\frac{\text{Re } H_{s0}^{m'\downarrow, i\uparrow}}{E_{i\uparrow} - E_F} V_{xy}^{i\uparrow, m\uparrow} + \frac{\text{Re } H_{s0}^{m\uparrow, i\downarrow}}{E_{i\downarrow} - E_F} V_{xy}^{i\downarrow, m'\downarrow} \right] \frac{|\xi_{\mathbf{k}}|^2}{4\hbar\omega} + \left[\frac{\text{Im } H_{s0}^{m'\downarrow, i\uparrow}}{E_{i\uparrow} - E_F} V_{xy}^{i\uparrow, m\uparrow} + \frac{\text{Im } H_{s0}^{m\uparrow, i\downarrow}}{E_{i\downarrow} - E_F} V_{xy}^{i\downarrow, m'\downarrow} \right] \text{Im } \xi_{\mathbf{k}} \right\}, \quad (17)$$

where

$$V_{xy}^{i\sigma, j\sigma} \equiv \frac{v_x^- v_y^{i\sigma, j\sigma} - v_y^- v_x^{i\sigma, j\sigma}}{|[v^- v^+]|}, \quad H_{s0}^{i\sigma, j\sigma} \equiv \langle \mathbf{k} i\sigma | \hat{H}_{s0} | \mathbf{k} j\sigma \rangle.$$

The notation in Eq. (17) is the same as in Eq. (15). The antisymmetry of $\text{Im } \sigma_{xy}(\omega)$ relative to the transposition $x \rightleftharpoons y$ is obvious. In the determination of Eq. (17) we allowed

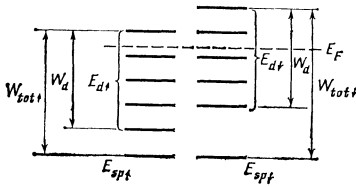


FIG. 2. Model of the valence band which explains quantitatively the behavior of $\text{Im } \sigma_{xy}(\omega)$ in the visible and ultraviolet parts of the spectrum.

not only for hybridization due to the SOI of the $m \uparrow$ and $m' \downarrow$ bands, but also for mixing of the remaining $i\sigma$ bands with the $m \uparrow$ and $m' \downarrow$ bands (this is again due to the SOI). Clearly, the effect described by Eq. (17) is of the order of the fraction $\xi / \Delta E_{\lambda\lambda'}$ of the corresponding contribution to the diagonal component of $\text{Re } \sigma_{xx}^{\text{II}}(\omega)$ in Eq. (15). Naturally, the proportions of the various contributions of these types to the diagonal components of $\text{Re } \sigma_{xx}(\omega)$ are valid also for the corresponding contributions to the off-diagonal components of the conductivity tensor.

We shall conclude this section by considering the problem of interpretation of the sign of $\text{Im } \sigma_{xy}(\omega)$.

The behavior of the frequency dependence of the sign of $\text{Im } \sigma_{xy}(\omega)$ requires a separate discussion because of the alternating-sign nature of the ratio

$$\text{Im } \sigma_{xy}(\omega) / (\text{Re } \sigma_{xx}^{\uparrow}(\omega) - \text{Re } \sigma_{xx}^{\downarrow}(\omega)).$$

We shall simplify the analysis by adopting the following model of the valence band (Fig. 2): the first subbands are of the sp type and the $1 \uparrow$ and $1 \downarrow$ bands practically coincide because of the smallness of the exchange splitting of the sp subband; there are then five d subbands with the up spin and the average interval $W_d/4$, as well as five d bands with the down spin, which are displaced from the latter by the exchange splitting energy Δ_{xc}^d of the d bands. The Fermi level of the investigated metals lies in the upper half of the valence band. It is clear from Eq. (12) that the sign of $\text{Im } \sigma_{xy}(\omega)$ can be represented by the following simplified expression

$$\text{sign}[\text{Im } \sigma_{xy}(\omega)] \sim \text{sign} \sum_{\sigma m m'} \sum_{\lambda} \left[\frac{L_{\lambda m'}^z}{E_{m'\lambda}} + \frac{L_{\lambda m}^z}{E_{m\lambda}} \right] S(\omega), \quad (18)$$

where

$$S(\omega) \equiv \text{Re } \sigma_{xx}^{\uparrow}(\omega) - \text{Re } \sigma_{xx}^{\downarrow}(\omega),$$

i.e., the sign of $S(\omega)$ depends on the projection of the spin σ for which the contribution to the conductivity is maximal at the selected frequency. Equation (18) is simplified by dropping the dependences of the momentum operator on the matrix elements (which represents the approximation of constant matrix elements), which is more or less justified at frequencies outside the infrared range. The position of the occupied state m' relative to the unoccupied state m determines the frequency ω at which the sign of $\text{Im } \sigma_{xy}(\omega)$ is investigated. Clearly, among the bands which are mixed with λ , the main role in determination of the sign of $\text{Im } \sigma_{xy}$ is played primarily by the term in Eq. (18) for the bands closest to m' , whereas in the second term the bands closest to m predominate. Moreover, we have to allow for the fact that the matrix elements $L_{\lambda m'}^z$ and $L_{\lambda m}^z$ of the SOI are diagonal in terms of the orbital quantum numbers l, l' , i.e., $(L^z)_{ll'} \sim \delta_{ll'}$.

Therefore, the sign of $\text{Im } \sigma_{xy}(\omega)$ is governed, on the one hand, by the type (based on the spin projection) of transition, i.e., by the sign of $S(\omega)$, and on the other by the nature and degree of interband hybridization (in terms of the orbital quantum numbers) governing the selection rules for $L_{\lambda m}^z$. Both these factors are practically independent of the crystal symmetry. This is confirmed by the complex behavior of $\text{sign}[\text{Im } \sigma_{xy}(\omega)]$ at all the investigated frequencies lying outside the infrared range and, in particular, by the reversal of the sign of

$$\text{Im } \sigma_{xy}(\omega) / (\text{Re } \sigma_{xx}^{\uparrow}(\omega) - \text{Re } \sigma_{xx}^{\downarrow}(\omega))$$

at photon energies $\hbar\omega \sim W_d$ observed for all the investigated metals. The fact that this applies to all metals is not accidental. In view of the practically complete filling of the valence subband with the up spin and the difference between the widths between the valence bands with the up spin $W_{\text{tot}\uparrow}$ and the down spin $W_{\text{tot}\downarrow}$ ($W_{\text{tot}\uparrow} - W_{\text{tot}\downarrow} \approx 2\Delta_{xc}^d$), the sign of $S(\omega)$ behaves as follows:

- 1) $\hbar\omega < W_d, S(\omega) < 0$ (spin down transitions predominate);
- 2) $W_d < \hbar\omega < \frac{1}{2}(W_{\text{tot}\uparrow} + W_{\text{tot}\downarrow}), S(\omega) > 0$ (spin up transitions predominate);
- 3) $\frac{1}{2}(W_{\text{tot}\uparrow} + W_{\text{tot}\downarrow}) < \hbar\omega < W_{\text{tot}\uparrow}, S(\omega) < 0$ (spin down predominate).

Now we can use Eq. (18) to follow the frequency dependence of the sign of $\text{Im } \sigma_{xy}(\omega)$. If $\hbar\omega < W_d$, then Eq. (18) is dominated by the m and m' bands only of the d type ($m = 5_{1,1}, 6_{1,1}, m' = 2_{1,1}, 4_{1,1}, 5_{1,1}$), and the terms with $\lambda = 1$ (for a band of the sp type) can be dropped because $L_{sd} \ll L_{d'd}$. If $W_d < \hbar\omega < W_{\text{tot}\uparrow}$ then in Eq. (18) we can assume that $m' = 1_{1,1}, m = 6_{1,1}$ and then, since the bands $\lambda = 2_{1,1}$ and $\lambda = 5_{1,1}$ are the nearest to m and m' , the dominant term is the second one in Eq. (18) and it contains L_{56}^z (because $L_{21}^z \ll L_{56}^z$). Consequently summing of the terms $1/E_{m'\lambda}$ and $1/E_{m\lambda}$ in Eq. (18) and inclusion of the contributions of the various types of [with different signs of $S(\omega)$] yields the following frequency dependence of $\text{sign}[-\text{Im } \sigma_{xy}(\omega)]$ (Fig. 3):

- 1) $\frac{2}{3}W_d < \hbar\omega < \frac{3}{4}W_d, \text{sign}[-\text{Im } \sigma_{xy}(\omega)] > 0$;
- 2) $\frac{3}{4}W_d < \hbar\omega < W_d, \text{sign}[-\text{Im } \sigma_{xy}(\omega)] \sim 0$;
- 3) $W_d < \hbar\omega < \frac{1}{2}(W_{\text{tot}\uparrow} + W_{\text{tot}\downarrow}), \text{sign}[-\text{Im } \sigma_{xy}(\omega)] > 0$;
- 4) $\frac{1}{2}(W_{\text{tot}\uparrow} + W_{\text{tot}\downarrow}) < \hbar\omega < W_{\text{tot}\uparrow}, \text{sign}[-\text{Im } \sigma_{xy}(\omega)] < 0$.

However, it should be pointed out that in the infrared range when $\hbar\omega \sim 2\xi$ the details of the energy band structure have a strong influence on the sign of $\text{Im } \sigma_{xy}$: the predominant nature (in respect of the spin) of the transition in the case of mechanism I, the projection of the spin of the nearest "third" band in mechanisms II, III, etc. For this reason we

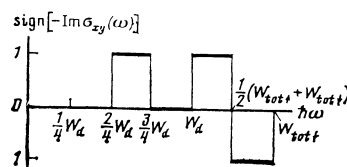


FIG. 3. Qualitative behavior of the sign of $\text{Im } \sigma_{xy}(\omega)$ in the visible and ultraviolet parts of the spectrum.

can hardly expect any universality of the behavior of the sign of $\text{Im } \sigma_{xy}(\omega)$ in this part of the spectrum.

3. ANALYSIS OF THE RESULTS OF NUMERICAL CALCULATIONS. COMPARISON WITH EXPERIMENTAL DATA

The above analysis is sufficient to give some ideas on the main features of the frequency dependence of $\sigma_{xy}(\omega)$. A calculation of $\sigma_{xy}(\omega)$ from first principles makes it possible to make these ideas more specific and to review both general and individual (for each metal) features of $\sigma_{xy}(\omega)$, to relate them to details of the band structure, and to compare the theoretical results with the experimental data. We shall report such calculations for Fe (bcc), Co (fcc), and Ni (fcc) with the magnetization directed so that $\mathbf{M} \parallel [001]$. Our calculations were carried out using Eqs. (4) and (5) with the wave functions and electron spectrum calculated by the LMTO method¹¹ within the framework of the theory of the functional of the local electron and spin densities.¹² In the main part of the optical spectrum the calculations were carried out at 525 K points in 1/16th part of the Brillouin zone, whereas in the infrared range we used a smaller mesh corresponding to about 5000 points in 1/16th part of the Brillouin zone. In other respects these calculations did not differ from those reported in our earlier papers.¹³

We shall begin an analysis of the main features of the frequency dependence of the conductivity tensor $\sigma_{\alpha\beta}(\omega)$ from the infrared part of the spectrum. As pointed out in Sec. 2, the dependence on the spin moment μ may be dominated by

different interband transition mechanisms. In the case of Fe and Co, where $2\Delta_{xc} \gg 2\bar{\xi}$ (large spin moment) the main contribution to $\sigma_{\alpha\beta}(\omega)$ comes from the vicinity of intersection between bands with opposite directions of the spin (mechanism II). We can easily from Fig. 4a that in the case of Fe such parts of the \mathbf{k} space consist of regions in the vicinity of lines of intersection of electron spheres with an electron surface centered at the point Γ and lines of intersection of hole pockets with an octahedron centered on H . Interband transitions in these parts of the Brillouin zone give rise to peaks of $\text{Im } \sigma_{xy}(\omega)$ at energies $\hbar\omega \sim 2\bar{\xi}$, which is 0.15 eV for iron and 0.17 eV for cobalt (Ref. 5). For comparison, Fig. 6 shows the $\text{Re } \sigma_{xx}(\omega)$ curves found allowing for and ignoring the SOI. The dominant role of the SOI in the formation of anomalies is quite obvious.

In the case of Ni, when $2\Delta_{xc} \sim 2\bar{\xi}$ and the spin moment is relatively small ($\mu = 0.55 \mu_B$) these lines of intersection of the Fermi surfaces with different spin directions are completely absent (Fig. 4b). As pointed out in Sec. 2, in this situation the transitions between the exchange-split bands ($6\uparrow, 6\downarrow$ in Ni) with characteristic energies $\hbar\omega \sim 2(\Delta_{xc}^2 + |\xi|^2)^{1/2}$ (mechanism III) become important.

Consequently, transitions in the part of the \mathbf{k} space limited by the surfaces $e_{6\uparrow}$ and $e_{6\downarrow}$ lead to the formation of a peak on the $\text{Re } \sigma_{xx}(\omega)$ and $\text{Im } \sigma_{xy}(\omega)$ curves at $\hbar\omega \approx 0.26$ eV, which is quite clear from Figs. 5 and 6. However, the experimental anomaly occurs at $\hbar\omega \approx 0.30$ eV (Ref. 3), which shows that $2\Delta_{xc} \approx 0.24$ eV at the Fermi level on condition that $2|\xi| = 0.18$ eV. It should be noted that in nonrelativistic calculations we find that the $\text{Re } \sigma_{xx}(\omega)$ curve has an anomaly at $\hbar\omega \approx 0.1$ eV, which is due to transitions in the part of the \mathbf{k}

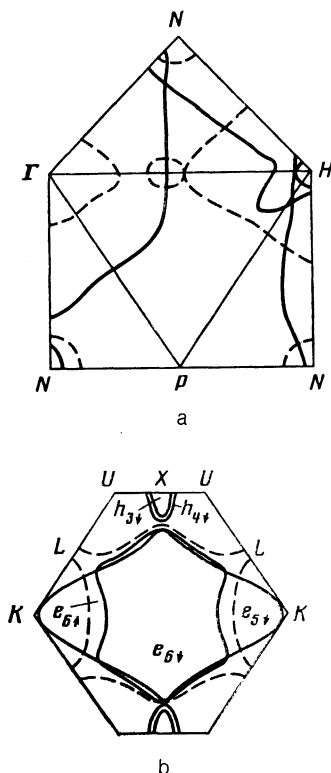


FIG. 4. Parts of the Fermi surface of Fe (a) and of Ni (b). The dashed curves represent the sheets with the up spin and the continuous curves represent the sheets with the down spin. The figure shows also the lines of intersection (Fe) and reasons for approach of the Fermi sheets with opposite spins (Ni, sheets $e_{6\uparrow}$ and $e_{6\downarrow}$), the vicinities of which make the maximum contribution to $\sigma_{\alpha\beta}(\omega)$ at photon energies $\hbar\omega \sim 2\bar{\xi}$.

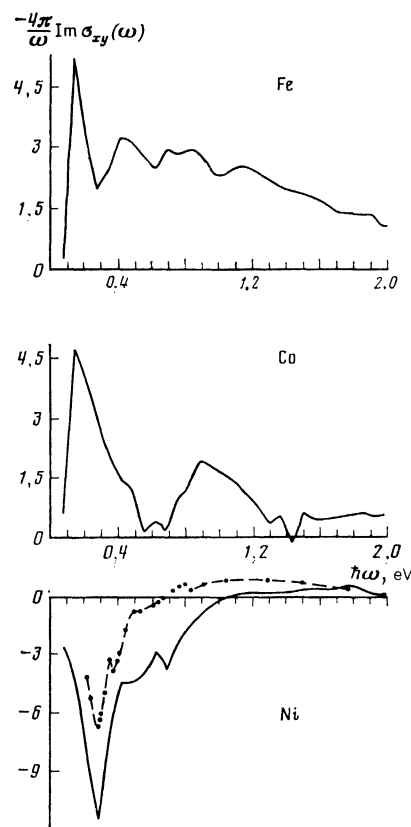


FIG. 5. Frequency dependence of $-(4\pi/\omega)\text{Im } \sigma_{xy}(\omega)$ in the infrared range. The points are the experimental values taken from Ref. 3.

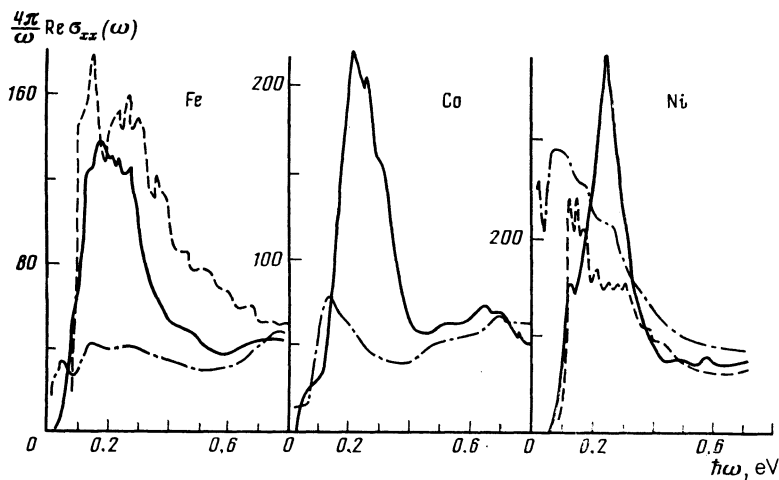


FIG. 6. Frequency dependence of $(4\pi/\omega)\text{Re}\sigma_{xx}(\omega)$ in the infrared range. The continuous curves allow for the spin-orbit interaction, the chain curves ignore this interaction, and the dashed curves give the experimental results obtained for Fe (Re f. 8) and for Ni (Re f. 23).

space bounded by e_{61} and e_{51} (mainly along the ΓU direction).

A negative peak at $\hbar\omega = 0.75$ eV (Fig. 5) in the case of Ni is due to transitions mainly in the vicinity of the directions ΓK and ΓW . A peak at this frequency occurs also on the $\text{Re}\sigma_{xx}(\omega)$ curve and it is due to spin down transitions, as demonstrated in Fig. 7. It would seem to us therefore that attribution of the exchange splitting to this singularity, made in Re f. 6, is unjustified. The experimental curve representing $\text{Im}\sigma_{xy}$ has a weak positive anomaly at this frequency.

In addition to the anomalous contributions to $\sigma_{\alpha\beta}(\omega)$ and $\hbar\omega \sim 2\bar{\xi}$, there are also the "normal" contributions (mechanism I), corresponding to transitions between bands with parallel spins and exhibiting monotonic variation (non-relativistic calculations, see Fig. 6). In the case of iron such transitions occur only in the vicinity of the point H , whereas in nickel they occur mainly along the ΓU direction.

In the infrared range there is a considerable variation in the behavior of $\sigma_{\alpha\beta}$ and in the interband transition mechanisms, whereas in the visible range the presence of two humps of $\text{Im}\sigma_{xy}(\omega)$ and reversal of the sign of $\text{Im}\sigma_{xy}(\omega)$ at the boundary of the visible spectrum are typical of all metals (Fig. 8). As pointed out in the preceding section, the behavior of

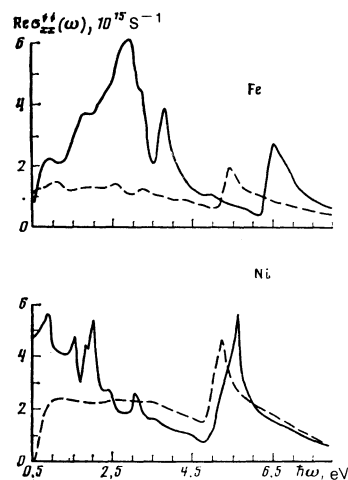


FIG. 7. Diagonal components of the conductivity with the up spin $\text{Re}\sigma_{xx}^+(\omega)$ (dashed curves) and with the down spin $\text{Re}\sigma_{xx}^-(\omega)$ (continuous curves).

$\text{Im}\sigma_{xy}(\omega)$ in the energy range $1\text{ eV} \lesssim \hbar\omega < 4\text{ eV}$ is approximately proportional to the difference $\text{Re}(\sigma_{xx}^+(\omega) - \sigma_{xx}^-(\omega))$, whereas $\text{Im}\sigma_{xy}(\omega)$ has anomalies at approximately the same frequencies as does $\text{Re}\sigma_{xx}^+(\omega)$ (Fig. 7), due to a practically complete filling of the valence band with the up spin. The occurrence of a negative peak in the ultraviolet part of the spectrum is also typical of the investigated metals and it is not accidental. It was reported in Re f. 14 that the $\text{Re}\sigma_{xx}(\omega)$ curve has two peaks in the near ultraviolet and these are due to $1\uparrow(sp\text{ type}) \rightarrow 6\uparrow(pd\text{ type})$ and $1\downarrow \rightarrow 6\downarrow$ transitions, i.e., the transitions between the outer valence bands, resulting from the difference between the exchange splitting of the sp and d bands. These peaks are separated by the average exchange splitting $2\Delta_{xc}^d$. This circumstance also creates a characteristic loop with reversal of the sign in the case of the

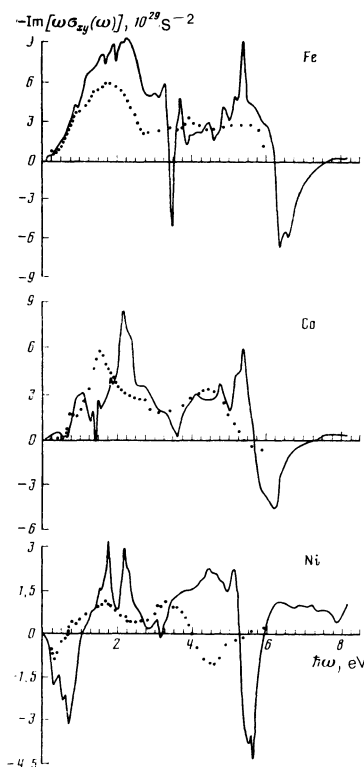


FIG. 8. Frequency dependence of $\text{Im}[\omega\sigma_{xy}(\omega)]$ in the visible and ultraviolet regions.

TABLE I. Width W_d of the d band and the exchange splitting $2\Delta_{xc}^d$ of the d bands of Fe, Co, and Ni.

	W_d, eV				$2\Delta_{xc}^d, eV$			
	band calc.	magneto-optic calc.	magneto-optic exp.	photo-emission exp.	band calc.	magneto-optic calc.	magneto-optic exp.	photo-emission exp.
Fe	4.8 (Δ)	4.8	4.3 [2]	~ 4.5 [21]	1.8 ($\Gamma_{25'}$)	$1.4+2\Delta_{xc}^s$	$1.8+2\Delta_{xc}^s$ [2]	2.0 ($\Gamma_{25'}$) [16] ~ 1.5 (P_i) [17] ~ 1.1
Co	4.5 (Δ)	4.5	3.9 (ihcp) [2]	(Δ, hcp) [20]	1.4 (Δ)	$1.2+2\Delta_{xc}^s$	$1.4+2\Delta_{xc}^s$ [2]	[17]
Ni	4.7 (L)	4.7	3.1 [2]	3.4 (L) [15]	0.65 (L_s)	$0.5+2\Delta_{xc}^s$	$0.9+2\Delta_{xc}^s$ [2]	0.33 (Δ) [18] 0.30 (L_s) [19]

Note. Here, $2\Delta_{xc}^s$ denotes the average exchange splitting of the sp bands ($\Delta_{xc}^s \ll \Delta_{xc}^d$).

$\text{Im } \sigma_{xy}(\omega)$ curve, as pointed out in Sec. 2. A positive peak of this loop corresponds to spin up transitions and a negative peak to the spin down transitions. The separation between the point of reversal of the sign and the negative peak is equal to half the exchange splitting Δ_{xc}^d .

In the case of Fe and Co the behavior of $\text{Im } \sigma_{xy}(\omega)$ is in agreement with the experimental results (Fig. 8). In the case of Ni the form of the $\text{Im } \sigma_{xy}(\omega)$ curve is very similar to that found experimentally, but the energy scale is extended by almost 40%. It follows from our earlier treatment of the main features of $\text{Im } \sigma_{xy}(\omega)$ that the most likely reason for this disagreement is the width of the d band which is too large. In fact, as demonstrated by the values in Table I, the width of the d band calculated using the theory of the functional of the local electron and spin densities agrees very well with the value W_d deduced from the calculated curve $\text{Im } \sigma_{xy}(\omega)$. On the other hand, the width of the d band found from the experimental $\text{Im } \sigma_{xy}(\omega)$ curve² agrees well with the results of photoemission investigations¹⁵ and both experimental values are very different from those found theoretically. In the case of the exchange splitting the situation is even more contradictory. The theoretical value of $2\Delta_{xc}$ for Ni is almost twice as large as the value deduced from photoemission investigations,^{18,19} but it is in reasonable agreement with the experimental value found from $\text{Im } \sigma_{xy}(\omega)$ (Ref. 2) although because of the smoothed-out nature of the experimental curve precision was not high. In the case of the other two metals, Fe and Co, we find that both W_d and $2\Delta_{xc}$ agree satisfactorily with the experimental data (Table I). The disagreement in the case of the electron structure of Ni has been discussed widely in the literature in connection with photoemission experiments.²² On the whole, this discrepancy is due to inadequate nature of the approximation of the local spin density in the case of Ni and the need to include corrections to the one-electron energies for this metal.

CONCLUSIONS

The investigation reported above demonstrates that suitably interpreted magneto-optic effects can give quite extensive information on the electron and particularly spin structure of ferromagnetic metals. It follows from an analytic treatment and from numerical calculations that the main

features of the magneto-optic and ordinary optical curves are closely related, but the former appear more strongly and they are more closely related to the spin structure, so that they should become the preferred instruments for investigation of this structure.

Among the more concrete results obtained in the present study is the conclusion that the investigated three mechanisms of interband transitions in the infrared part of the spectrum are quite universal. All these mechanisms give rise to such an anomaly at the frequency $\sim 2\xi$ so that the spin-orbit splitting can be deduced from magneto-optic curves. The same mechanisms should occur also in ferromagnetic compounds and in other ferromagnetic metals. The only difference is that the dependence on the spin moment and on the actual energy band structure is dominated by one or another mechanism. It seems to us that proportionality between the quantities $\text{Im } \sigma_{xy}(\omega)$ and $\text{Re}(\sigma_{xx}^l(\omega) - \sigma_{xx}^r(\omega))$ found in a wide range of frequencies is also quite universal. The anomalies at $\hbar\omega \sim W_d$, accompanied by a change of the sign of $\text{Im } \sigma_{xy}(\omega)$, may not be so universal because they are very closely connected with the specific electron structure of the $3d$ metals. We can assume however that in the case of ferromagnetic compounds and other ferromagnetic materials there are some analogous anomalies. We hope that the present work will help in interpretation of these effects.

The authors are grateful to G. S. Krinchik, E. A. Gan'shina and V. V. Losyakov for valuable comments in the course of our investigation.

¹P. N. Argyres, Phys. Rev. **97**, 334 (1955).

²G. S. Krinchik and V. A. Artem'ev, Zh. Eksp. Teor. Fiz. **53**, 1901 (1967) [Sov. Phys. JETP **26**, 1080 (1968)].

³G. S. Krinchik and G. M. Nurmukhamedov, Zh. Eksp. Teor. Fiz. **48**, 34 (1965) [Sov. Phys. JETP **21**, 22 (1965)].

⁴G. S. Krinchik and E. A. Gan'shina, Zh. Eksp. Teor. Fiz. **65**, 1970 (1973) [Sov. Phys. JETP **38**, 983 (1974)].

⁵J. L. Erskine and E. A. Stern, Phys. Rev. **B 8**, 1239 (1973).

⁶C. S. Wang and J. Callaway, Phys. Rev. **B 9**, 4897 (1974).

⁷H. S. Bennett and E. A. Stern, Phys. Rev. **137**, A448 (1965).

⁸V. P. Shirokovskii, M. M. Kirillova, and N. A. Shilkova, Zh. Eksp. Teor. Fiz. **82**, 784 (1982) [Sov. Phys. JETP **55**, 464 (1982)].

⁹L. D. Landau, E. M. Lifshitz, and L. P. Pitaevskii, *Electrodynamics of Continuous Media*, 2nd ed., Pergamon Press, Oxford (1984).

¹⁰B. R. Cooper, Phys. Rev. **139**, A1504 (1965).

¹¹O. K. Andersen, Phys. Rev. **B 12**, 3060 (1975).

- ¹²S. Lundqvist and N. H. March (eds.), *Theory of the Inhomogeneous Electron Gas*, Plenum Press, New York (1983).
- ¹³Yu. A. Uspenskii, E. G. Maksimov, S. N. Rashkeev, and I. I. Mazin, *Z. Phys. B* **53**, 263 (1983).
- ¹⁴S. V. Khalilov, S. N. Rashkeev, and Yu. A. Uspenskii, *Fiz. Tverd. Tela (Leningrad)* **29**, 1467 (1987) [*Sov. Phys. Solid State* **29**, 839 (1987)].
- ¹⁵D. E. Eastman, F. J. Himpsel, and J. A. Knapp, *Phys. Rev. Lett.* **40**, 1514 (1978).
- ¹⁶R. Feder, W. Gudat, E. Kisker, A. Rodriguez, and K. Schroder, *Solid State Commun.* **46**, 619 (1983).
- ¹⁷D. E. Eastman, F. J. Himpsel, and J. A. Knapp, *Phys. Rev. Lett.* **44**, 95 (1980).
- ¹⁸P. Heimann, F. J. Himpsel, and D. E. Eastman, *Solid State Commun.* **39**, 219 (1981).
- ¹⁹C. J. Maetz, U. Gerhardt, E. Dietz, A. Ziegler, and R. J. Jelitto, *Phys. Rev. Lett.* **48**, 1686 (1982).
- ²⁰F. J. Himpsel and D. E. Eastman, *Phys. Rev. B* **21**, 3207 (1980).
- ²¹M. Pessa, P. Heimann, and H. Neddermeyer, *Phys. Rev. B* **14**, 3488 (1976).
- ²²A. Liebsch, *Phys. Rev. B* **23**, 5203 (1981).
- ²³M. M. Kirillova, *Zh. Eksp. Teor. Fiz.* **61**, 336 (1971) [*Sov. Phys. JETP* **34**, 178 (1972)].

Translated by A. Tybulewicz